Equations for chromatographic peak modeling and calculation of peak area

ARTICLE *in* ANALYTICAL CHEMISTRY · AUGUST 1987

Impact Factor: 5.64 · DOI: 10.1021/ac00142a019

1 AUTHOR:

Joe P. Foley
Drexel University
108 PUBLICATIONS **3,279** CITATIONS

SEE PROFILE

(10) Dumasia, M. C.; Houghton, E. *Xenobiotica* **1981**, *11*, 323-331.
(11) Dumasia, M. C.; Houghton, E.; Bradley, C. V.; Williams, D. H. *Biomed. Mass Spectrom.* **1983**, *10*, 434-440.
(12) Vihko, R. *Acta Endocrinol. (Copenhagen), Suppl.* **1966**, *109*, 29.
(13) Berendsen, G. E.; Schoenmakers, P. J.; de Galan, L.; Vigh, G.; Varga-Puchony, Z.; Inczedy, J. *J. Liq. Chromatogr.* **1980**, *3*, 1669-1686.
(14) Simonian, M. H.; Capp, M. W. *J. Chromatogr.* **1984**, *287*, 97-104.
(15) Vestergaard, P. *Acta Endocrinol. (Copenhagen), Suppl.* **1978**, *217*, 96-120.
(16) Burstein, S.; Lieberman, S. *J. Am. Chem. Soc.* **1958**, *80*, 5235-5239.
(17) Tuinstra, L. G. M. Th.; Traag, W. A.; Keukens, H. J.; Van Mazijk, R. J. *J. Chromatogr.* **1983**, *279*, 533-542.
(18) Dumasia, M. C.; Houghton, E.; Sinkins, S. *J. Chromatogr.* **1986**, *377*, 23-33.

RECEIVED for review December 23, 1986. Accepted April 6, 1987. Financial support for this work was obtained from the Harry M. Zweig Memorial Fund, International Minerals and Chemicals Corp. (Terra Haute, IN), and the New York State Racing and Wagering Board.

Equations for Chromatographic Peak Modeling and Calculation of Peak Area

Joe P. Foley

Department of Chemistry, Louisiana State University, Baton Rouge, Louisiana 70803-1804

By use of the exponentially modified Gaussian (EMG) as the skewed model, empirical equations based on peak height, width, and asymmetry measurements have been developed for the accurate and precise calculation of peak area for symmetric (Gaussian) and skewed peaks. These equations are useful in determining whether or not an experimental chromatographic peak fits the Gaussian or EMG peak model. They can also be used in quantitative analyses when electronic integration is precluded by peak overlap, base-line drift, etc. or when electronic integration is unavailable. By use of the area equations, 40 liquid chromatographic peaks were tested and 90% were found to fit the Gaussian or EMG model.

Quantitative peak shape analysis is important in many areas of analytical chemistry. In chromatography, as noted recently by Dezaro et. al (*1*), the degree and nature of peak asymmetry are indicative of problems with stationary phase kinetics, thermodynamics, or extracolumn effects.

Two approaches have traditionally been taken for chromatographic peak characterization. The first approach assumes a Gaussian peak shape so that a parameter of interest, e.g., plant count, may be calculated from graphically measurable parameters. The second approach employs statistical moment calculations following data acquisition and makes no assumptions about peak shape. Both of these approaches have serious drawbacks: the Gaussian approach is grossly inaccurate, and the data acquisition/moment approach is frequently imprecise and moderately inaccurate due to noise (*2-5*), uncertainties in peak stop/start assignments (*4*, *6*, *7*), and base-line drift (*2*, *8*). In addition, the higher moments are especially sensitive to peak tailing (*2*). A final drawback of the moment method is that it is not available in every laboratory.

Recently some empirical methods based on graphically measurable parameters were introduced (*9*, *10*) for the characterization of chromatographic peaks. They are accurate for both Gaussian and tailed peaks, assuming the tailed peaks fit a widely accepted exponentially modified Gaussian (EMG) peak-shape model.

Although the EMG function is usually an adequate model for tailed chromatographic peaks (*11*), the adequacy should always be verified before the EMG model is employed. The previous graphical methods for testing the fit of peaks to the EMG model require a comparison of values of several peak parameters at three peak height fractions (*9*, *10*). Although these peak-testing methods are adequate in most cases, they may lack the precision to reject marginal peaks. In addition, these methods require numerous calculations of several parameters and are thus somewhat impractical.

In this paper we report equations for the calculation of the peak area of Gaussian and EMG peaks. These equations can be used to test more accurately and precisely the fit of real peaks to the Gaussian or EMG model. They can also be used to accurately quantitate Gaussian and EMG peaks when peak overlap, base-line errors, noise, etc. preclude electronic integration or when electronic integration is unavailable or is suspect.

EXPERIMENTAL SECTION

Computations. Either an Apple II+ or an Apple Macintosh computer was used for all calculations. Programs were written in BASIC.

EMG Peak Generation. The exponentially modified Gaussian (EMG) function results from the convolution of a Gaussian function and an exponential decay function and can be expressed in a variety of ways (*12-14*). The specific form we used was

$$\mathrm{EMG}(t) = A/\tau \exp[(1/2) \times (\sigma_G/\tau)^2 - (t - t_G)/\tau] \int_{-\infty}^{Z} \exp(-y^2/2)/(2\pi)^{1/2}\, dy \quad (1)$$

where A is the peak area, t_G and σ_G are the retention time and standard deviation of the Gaussian function, τ is the time constant of the exponential decay function, and $z = (t - t_G)/\sigma_G - \sigma_G/\tau$. The integral in eq 1 was evaluated by use of an accurate polynomial approximation (*11*). Note that the ratio τ/σ_G is a fundamental measure of peak asymmetry. As τ/σ_G increases, the tailing of the chromatographic peak increases. As τ/σ_G approaches 0, the resulting peak approaches that of a Gaussian.

Values of $A = 1$, $t_G = 100$, and $\sigma_G = 5$ were used in eq 1 for peak generation. The τ/σ_G ratio was varied from 0.3 to 4.2 in 0.1 increments producing data equivalent to 40 peaks. A search algorithm described previously (*11*) was used for the measurement of the retention time, peak height, width, and asymmetry at several peak height fractions (0.1, 0.25, 0.3, 0.5, and 0.75). These parameters are illustrated in Figure 1 for an EMG peak with $\tau/\sigma_G = 2$.

Empirical Area Equations. Equations for the accurate calculation of peak area for a wide range of symmetric (Gaussian) and tailed (EMG) peaks were obtained by the least-squares fitting of A_{true}/A_G vs. b/a from $\tau/\sigma_G = 0.3$-4.2, where A_{true} is the area from eq 1, b/a is the empirical asymmetry factor, and A_G is the area calculated by using the Gaussian equation (*15*)

$$A_G = C_r h_P W_r \quad (2)$$

0003-2700/87/0359-1984$01.50/0

Table I. Peak Area Equations for Gaussian and Exponentially Modified Gaussian (EMG) Peaks[a]

equation	% RE[b]	% RSD[c]
$A = 0.586h_pW_{0.1}(b/a)^{-0.133}$	±0.50	1.44
$A = 0.753h_pW_{0.25}$	−1.0, +0.6	1.41
$A = 1.07h_pW_{0.5}(b/a)^{+0.235}$	−1.2, +1.0	1.49
$A = 1.64h_pW_{0.75}(b/a)^{+0.717}$	−1.1, +0.6	2.01

[a] A is area of peak, h_p is peak height, W is width of peak at the designated peak height fraction given by the subscript, and b/a is an asymmetry factor measured at the same peak height fraction as the width. See Figure 1. [b] Largest relative error of the area equations over the interval $0 \leq \tau/\sigma \leq 4.2$ $\{1.00 \leq (b/a)_{0.1} \leq 3.60\}$, expressed as a percentage. [c] Relative standard deviation (RSD) of the area measurement, expressed as a percentage and predicted from error propagation (eq 5), assuming RSDs of 1%, 1%, and 2% for h_p, W, and b/a. Note that for many data acquisition systems the precision of h_p, W, and b/a can be better than what we have assumed.

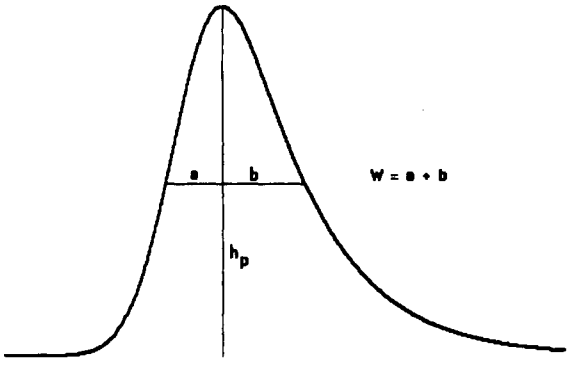

Figure 1. Graphical parameters of an exponentially modified Gaussian (EMG) peak with $\tau/\sigma_G = 2$, shown here for peak height fraction $r = 0.5$: W, peak width; h_p, peak height, and b/a, asymmetry factor. These parameters are used in the area equations in Table I.

where A_G is the peak area, r is the peak height fraction, $C_r = (1/2)[\pi/\ln(1/r)]^{1/2}$, h_p is the peak height, and W_r is the peak width at the specified peak height fraction. The general form of the fitted equations was

$$A_{true}/A_G = C_1(b/a)^{C'} \quad (3)$$

where C_1 and C' are fitting constants, and b/a is the asymmetry of the peak at the same peak height fraction as W_r of eq 2. Substitution of eq 2 into eq 3, followed by the dropping of the subscript "true" from A_{true} and rearrangement, yields the empirical area equations reported in Table I

$$A = Ch_pW_r(b/a)^{C'} \quad (4)$$

where $C = C_rC_1$.

Experimental Peak Modeling. Experimental chromatographic peaks were obtained by injecting dilute solutions of reagent grade acetophenone, anisole, and toluene onto several reversed-phase columns from different manufacturers, using either acetonitrile/water or methanol/water as the mobile phase, in proportions (usually ≥2:1) that gave k' values of 2–6. The liquid chromatograph used in the study was a Varian Model 5000, which incorporated a Rheodyne Model 7125 injector with 20-μL loop, a Varian column heater block set a few degrees above ambient for temperature stability, and a Varian UV detector (254 nm) with a time constant of ca. 1.1 s. A strip chart recorder was used to record all chromatograms. All peak height, width, and asymmetry measurements (see Figure 1) of the experimental chromatographic peaks were made manually, following guidelines recommended previously (*10*).

RESULTS AND DISCUSSION

Graphical Parameters. An exponentially modified Gaussian (EMG) peak (eq 1) with a value of $\tau/\sigma_G = 2$ is shown in Figure 1. The measurements of the graphical parameters needed for calculation of peak area are illustrated at half height.

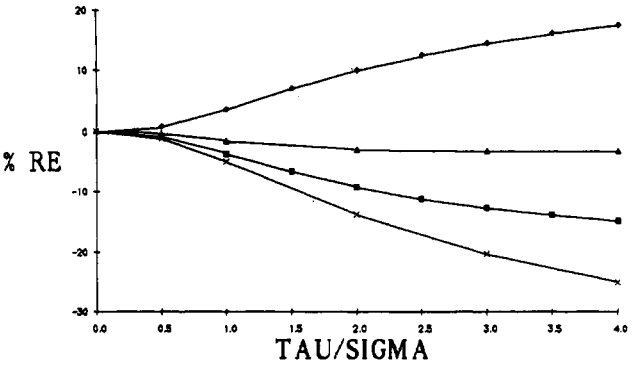

Figure 2. Error of Gaussian equations (eq 2, text) for the calculation of peak area of skewed (EMG) peaks at peak height fractions 0.10 (●), 0.3 (▲), 0.5 (■), and 0.75 (×).

Gaussian Area Equations. The relative error (RE) of the Gaussian area equations (eq 2) for a wide range of EMG peaks is shown in Figure 2. The inaccuracy of the Gaussian equations is not surprising since they do not account for peak asymmetry. Whereas the Gaussian area equation based on $W_{0.1}$ measurements (eq 2, $C_r = 0.584$) *over*estimates EMG peak areas, the Gaussian equations based on $W_{0.3}$, $W_{0.5}$, and $W_{0.75}$ measurements *under*estimate EMG peak areas by successively greater amounts. Due to a fortuitous cancellation of error, the Gaussian equation at $r = 0.25$ (not shown in Figure 2) is accurate to within 1% for the entire range of EMG peaks.

Empirical Area Equations. The least-squares fitting procedure described in the Experimental Section was used to obtain empirical area equations (eq 4) at peak height fractions $r = 0.1$, 0.3, 0.5, and 0.75. Due to a poorer fit, the equation at $r = 0.3$ was somewhat less accurate and was not considered further. The remaining equations, along with the Gaussian equation at $r = 0.25$, are listed in Table I. The accuracy is stated in terms of the maximum relative error observed over 0.1 intervals for the τ/σ_G range of 0–4.2. The precision is given as the relative standard deviation, calculated according to the error propagation equation

$$s_A/A = [(s_{h_p}/h_p)^2 + (s_w/W)^2 + C'^2(s_{b/a}/(b/a))^2]^{1/2} \quad (5)$$

where s represents standard deviation and C' is the constant from eq 4. As shown in Table I, the accuracy and precision of all the equations are within 1% and 2%, respectively.

Applications of the Empirical Area Equations. The accurate calculation of the areas of ideal and skewed peaks via the equations in Table I will be helpful both in quantitative analyses and in peak modeling studies.

For quantitative analyses, the equations in Table I provide a practical means for accurately measuring peak areas when electronic integration is not available or for judging the reliability of the electronic data acquisition/integration when such instrumentation *is* available. For example, a significant difference between the peak area measured electronically and the peak measured manually via an equation in Table I may indicate that an inappropriate value had been used for one or more of the electronic integration parameters (slope sensitivity, peak threshold, etc.). In other instances, the equations may occasionally prove to be more reliable than electronic data acquisition/integration because of the latter's susceptibility to noise (*2–5*), uncertainties in peak stop/start assignments (*4, 6, 7*), and base-line drift (*2, 8*). Finally, as we discuss in a separate report (*16*), the equation in Table I at $r = 0.75$ can be used either by itself or in conjunction with electronic integration to provide improved quantitation for overlapping symmetric and tailed peaks.

In peak modeling studies (vide infra), the area equations in Table I can be used to test unknown peaks for their fit to the Gaussian or EMG model. The goodness of fit is judged

Table II. Area Calculations for Different Types of Peaks of Unit Area Using Equations in Table I

peak	$r = 0.1$[a]	$r = 0.25$	$r = 0.5$	$r = 0.75$
Gaussian	1.00	1.00	1.01	0.99
EMG ($\tau/\sigma_G = 2$)	1.00	0.99	0.99	0.99
triangle[b]	0.96	1.13	1.26	1.35
Lorentzian	1.12	0.83	0.68	0.60
gamma[c]	0.91	1.00	1.10	1.20
beta[d]	0.89	1.00	1.12	1.21

[a] Peak height fraction. [b] Triangle with an asymmetry factor (b/a) of 2 at all peak height fractions. [c] Probability density function for a gamma type random variable with $\alpha = 4$, $\beta = 1$. See ref 17. [d] Probability density function for a beta type random variable with $\alpha = 6$, $\beta = 3$. See ref 17. This function was reflected about the y axis for use in this study.

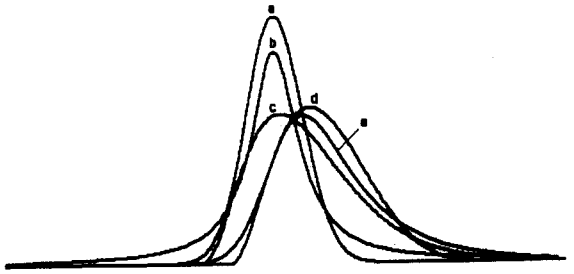

Figure 3. Several types of symmetric and asymmetric peaks on which the area equations in Table I were tested: Gaussian (a), Lorentzian (b), inverted beta (c), gamma (d), EMG (e).

by the consistency of the calculated areas. Although similar approaches (*9*, *10*) which compare values of σ_G, M_2, and τ (or τ/σ_G) are adequate for testing unknown peaks, the use of the area equations is preferred for three reasons: First, the equations for peak area are more accurate and precise than present equations for σ_G, M_2, and τ (or τ/σ_G), particularly for slightly skewed peaks (small values of τ/σ_G). Second, the area method is simpler in that it requires a comparison of values for only one parameter, peak area, whereas the previous methods require a comparison of values for three parameters. Third, a separate test based on width ratios is not needed for testing symmetric peaks for their resemblance to a Gaussian.

Distinguishing between Gaussian/EMG Peaks and Other Types of Peaks. With consistency of peak area as our test criterion, the equations in Table I can be used to distinguish between Gaussian/EMG peaks and other types of symmetric and asymmetric peaks. That is, for a given peak in question, if consistent areas are obtained by using all four equations (based on width and asymmetry measurements at four *different* peak height fractions), then the peak is either a Gaussian peak (if symmetric) or an EMG peak (if asymmetric). Conversely, if consistent areas are not obtained, the peak is neither a Gaussian nor an EMG peak. Note that the degree of consistency required will depend in part on the limits of experimental error.

The effectiveness of this area test in distinguishing between Gaussian/EMG peaks and other types of symmetric and asymmetric peaks is shown in Table II, where areas calculated by using each of the four equations in Table I are reported for six different types of peaks. The peaks themselves are illustrated in Figure 3.

As shown in Table II, all four areas calculated for the Gaussian and EMG peaks are consistent to within ±1%, whereas the areas calculated for each of the four non-Gaussian/EMG peaks are extremely inconsistent, with variations in area ranging from 29% for the beta peak to 52% for the Lorentzian peak. While it is not surprising that our area test works so well for the triangular and Lorentzian peaks, the ability of the area test to distinguish the gamma and beta peaks from the Gaussian/EMG peaks is noteworthy, since the gamma and beta peaks closely resemble the EMG peak. In summary, the data of Table II show our area test to be a viable, practical method for distinguishing between Gaussian/EMG peaks and other types of peaks.

Table III. Peak Modeling Results for Reversed-Phase Liquid Chromatographic Peaks[a]

peak grouping	no. of peaks	% of exptl peaks that fit the model[b] within 10%	within 5%
solutes			
acetophenone	10	100	100
anisole	10	100	80
toluene	20	100	90
columns[c]			
C18, 1	11	100	91
C18, 2	6	100	83
C18, 3	5	100	100
C8	10	100	90
C1	2	100	50
PS-DVB	6	100	100
total[d]	40	100	90

[a] Conditions varied according to the test solutes. Mobile phases employed were those recommended by the manufacturer. Data in the grouping by solute are necessarily duplicated in the grouping by column. [b] Defined as whether or not the areas calculated via the equations in Table I fell within the specified range. [c] C18, C8, and C1 refer to conventional hydrophobic bonded phases, i.e., hydrocarbon chains of 18, 8, and 1 carbon unit bonded to a silica support. PS-DVB refers to a polystyrene–divinylbenzene macroporous copolymer phase. [d] Data from the grouping by solute are duplicated in the grouping by column.

Modeling of Experimental Chromatographic Peaks. Although the Gaussian and EMG models have been shown to adequately represent chromatographic peaks under most conditions (*11*), we thought it appropriate to test some experimental peaks ourselves, using the area equations we have developed. As described in the Experimental Section, 40 liquid chromatographic peaks were tested. The results are summarized in Table III.

All of the peaks examined were at least slightly asymmetric $\{(b/a)_{0.1} \geq 1.10\}$, and were found to fit the EMG model to within 10%. Ninety percent of the peaks fit the EMG model to within 5%. As shown in Table III, no significant differences were observed among the three solutes or six columns tested.

Peak Characterization. Once the fit of the unknown peaks to the Gaussian or EMG model has been confirmed by the area test using the equations in Table I, the equations reported previously by Foley and Dorsey (*9*) can be used to measure such chromatographic parameters as column efficiency (theoretical plates), peak variance (M_2), and statistical moments or related parameters. These equations have been verified both theoretically and experimentally by other researchers (*18–20*). Alternatively, for the calculation of statistical moments, the equations reported by Anderson and Walters (*8*) may be used.

Accuracy of the Gaussian Area Equation at $r = 0.25$ for non-Gaussian/EMG Peaks. A result I did not anticipate was the accuracy of an unmodified Gaussian area equation (Table I, $r = 0.25$) for several other types of peaks. It should be emphasized that this accuracy of this specific Gaussian equation is strictly fortuitous and that other Gaussian area equations will not be accurate for non-Gaussian peaks. Nevertheless, this Gaussian equation is accurate for a wide range of EMG peaks, as shown in Table I, and it is also accurate for some types of gamma and beta peaks, as shown in Table II. Further study is warranted, but it appears that this equation (Table I, $r = 0.25$) will be accurate for many

types of asymmetric peaks not limited to the EMG model.

Nonchromatographic Peak Profiles. The EMG model, and hence, the empirical equations developed from this model [reported here and elsewhere (*8*, *10*)], may also be applicable to nonchromatographic peaks. For example, many peaks reported in flow injection analysis and in graphite furnace atomic spectrometry bear a strong resemblance to EMG peaks (for example, see ref 21-26). In one preliminary study, application of the area test described in this report showed that nearly half of the graphite furnace atomic fluorescence peaks are examined were adequately modeled by the EMG function (*26*). Thus, although not yet justified on theoretical grounds, the EMG model and empirical equations should be of great benefit for characterizing many types of nonchromatographic peaks.

Future Studies. We have reported empirical equations based on peak height, width, and asymmetry for the accurate calculation of peak area for Gaussian and EMG peaks. These equations are useful in quantitative analysis and in the modeling of symmetric and tailed chromatographic peaks. They can easily be incorporated into the software of computing integrators and data acquisition systems. In the future, we plan to examine the applicability of the empirical area equations and empirical statistical moment equations for the detection and characterization of coeluting and partially resolved peaks.

LITERATURE CITED

(1) Dezaro, D. A.; Floyd, T. R.; Raglione, T. V.; Hartwick, R. A. *Chromatogr. Forum* **1986**, *1*, 34-37.
(2) Grushka, E.; Myers, M. N.; Schettler, P. D.; Giddings, J. C. *Anal. Chem.* **1969**, *41*, 889-892.
(3) Petitclerc, T.; Guiochon, G. *J. Chromatogr. Sci.* **1976**, *14*, 531-535.
(4) Chesler, S. N.; Cram, S. P. *Anal. Chem.* **1971**, *43*, 1922-1933.
(5) Yau, W. W. *Anal. Chem.* **1977**, *49*, 395-398.
(6) Kirkland, J. J.; Yau, W. W.; Stoklosa, H. J.; Dilks, C. H. *J. Chromatogr. Sci.* **1977**, *15*, 303-316.
(7) Rony, P. R.; Funk, J. E. *J. Chromatogr. Sci.* **1971**, *9*, 215-219.
(8) Anderson, D. P.; Walters, R. R. *J. Chromatogr. Sci.* **1984**, *22*, 353-359.
(9) Barber, W. E.; Carr, P. W. *Anal. Chem.* **1981**, *53*, 1939-1942.
(10) Foley, J. P.; Dorsey, J. G. *Anal. Chem.* **1983**, *55*, 730-737.
(11) Foley, J. P.; Dorsey, J. G. *J. Chromatogr. Sci.* **1984**, *22*, 40-46.
(12) Hanggi, D.; Carr, P. W. *Anal. Chem.* **1985**, *57*, 2394-2395.
(13) Delley, R. *Chromatographia* **1984**, *18*, 374-382.
(14) Delley, R. *Anal. Chem.* **1985**, *57*, 388.
(15) Ball, D. L.; Harris, W. E.; Habgood, H. W. *Sep. Sci.* **1967**, *2*, 81-99.
(16) Foley, J. P. *J. Chromatogr.* **1987**, *384*, 301-313.
(17) Mendenhall, W.; Scheaffer, R. L. *Mathematical Statistics with Applications*; Duxbury: North Scituate, MA, 1973; pp 128-131.
(18) Hayes, J. M.; Schwartz, H. E.; Vouros, P.; Karger, B. L.; Thruston, A. D.; McGuire, J. M. *Anal. Chem.* **1984**, *56*, 1229-1236.
(19) Bidlingmeyer, B. A.; Warren, F. V., Jr. *Anal. Chem.* **1984**, *56*, 1583A-1596A.
(20) Niessen, W. M. A.; van Vliet, H. P. M.; Poppe, H. *Chromatographia* **1985**, *19*, 357-363.
(21) Vanderslice, J. T.; Rosenfeld, A. G.; Beecher, G. R. *Anal. Chim. Acta* **1986**, *179*, 119-129.
(22) Tyson, J. F. *Anal. Chim. Acta* **1986**, *179*, 131-148.
(23) Leclerc, D. F.; Bloxham, P. A.; Toren, E. C., Jr. *Anal. Chim. Acta* **1986**, *184*, 173-185.
(24) Sturgeon, R. E.; Berman, S. S. *Anal. Chem.* **1985**, *57*, 1268-1275.
(25) Cedergren, A.; Frech, W.; Lundberg, E. *Anal. Chem.* **1984**, *56*, 1382-1387.
(26) Winefordner, J. D., University of Florida, personal communication, 1986.

RECEIVED for review December 1, 1986. Accepted April 17, 1987.

Determination of Parts-per-Billion Concentrations of Dioxane in Water and Soil by Purge and Trap Gas Chromatography/Mass Spectrometry or Charcoal Tube Enrichment Gas Chromatography

Paul S. Epstein,* Theresa Mauer, Michael Wagner, Susan Chase, and Betsy Giles

Clayton Environmental Consultants, Inc., Novi, Michigan 48050

Two methods for the determination of 1,4-dioxane in water have been studied. The first method is a heated purge and trap gas chromatography/mass spectrometry system following salting out with sodium sulfate. The second method is an adsorption on coconut-shell charcoal and solvent desorption with carbon disulfide/methanol followed by analysis of the desorbate by gas chromatography with flame ionization detection. The first method is also successful for the determination of 1,4-dioxane in solids and sediments. The second method is shown to be successful for 2-butanone, 4-methyl-2-pentanone, and butoxyethanol in water. The two methods are compared by analyzing 15 samples by both methods and achieving similar results.

The determination of 1,4-dioxane at parts-per-billion concentrations in water and soil samples presents difficulties because of the high water solubility of the compound. Friant and Suffert (*1*) have published a study that uses 1,4-dioxane as a model compound in the comparison of methods to improve the headspace analysis of organics in water. They reported a theoretical limit of detection of 740 ppb for 1,4-dioxane by a heated headspace method. Higher levels of 1,4-dioxane in water (1 ppm) are amenable to analysis by direct injection onto a Porapak Q column and detection by flame-ionization gas chromatography (GC-FID) (*2*).

Initial attempts to use the gas chromatography/mass spectrometry (GC/MS) purge and trap method (USEPA Method 624) based on the work of Bellar and Lichtenburg (*3*, *4*) were moderately successful. A limit of detection of 20 ppb was achieved. We undertook a study to see if we could either improve on the purge and trap method for this difficult to determine compound or develop an alternate method that would provide low limits of detection.

Recent articles on the use of graphitized carbon black for the enrichment of trace organics from water (*5*, *6*) indicated that we might be able to develop a similar analysis for the 1,4-dioxane. There is an established method (*7*) for the analysis of 1,4-dioxane in air. This method involves the adsorption of 1,4-dioxane onto coconut-shell charcoal and desorption with carbon disulfide and analysis by GC-FID. Two

0003-2700/87/0359-1987$01.50/0